Quantifying MLI Thermal Conduction in Cryogenic Applications from Experimental Data

R G Ross, Jr

Jet Propulsion Laboratory, California Institute of Technology
Pasadena, CA 91109 USA

Abstract: Multilayer Insulation (MLI) uses stacks of low-emittance metalized sheets combined with low-conduction spacer features to greatly reduce the heat transfer to cryogenic applications from higher temperature surrounds. However, as the hot-side temperature decreases from room temperature to cryogenic temperatures, the level of radiant heat transfer drops as the fourth power of the temperature, while the heat transfer by conduction only falls off linearly. This results in cryogenic MLI being dominated by conduction, a quantity that is extremely sensitive to MLI blanket construction and very poorly quantified in the literature. To develop useful quantitative data on cryogenic blanket conduction, multilayer nonlinear heat transfer models are used to analyze extensive heat transfer data measured by Lockheed Palo Alto on their cryogenic dewar MLI and measured by JPL on their spacecraft MLI. The data-fitting aspect of the modeling allows the radiative and conductive thermal properties of the tested blankets to be explicitly quantified. Results are presented showing that MLI conductance varies by a factor of 600 between spacecraft MLI and Lockheed's best cryogenic MLI.

1. Introduction

MLI is constructed using layers of double aluminized Mylar or Kapton separated by low-conductance spacers or stippled surfaces that prevent adjacent shield layers from directly contacting. The spacer layers also have the important function of providing for the evacuation of residual gas from between the shield layers when vacuum is applied. Though the spacers prevent the low-emittance shields from directly contacting, they themselves contact the aluminized layers and can lead to significant thermal conduction through the thickness of an MLI blanket [1]. This thermal conduction through the thickness of the MLI is highly sensitive to the compressive pressure squeezing the layers together and thus to the resulting layer density (N), which is described in terms of layers per unit blanket thickness. To achieve a low conductance blanket, any compressive force or blanket bending that pushes the layers together must be carefully minimized.

Historically, MLI performance has been modelled using the Lockheed equation first derived in a large multi-year MLI study conducted by Lockheed Palo Alto for NASA in the 1970s [2].

$$q = q_c + q_r = \frac{C_c N^{2.56} T_m}{n}(T_h - T_c) + \frac{C_r \epsilon_o}{n}(T_h^{4.67} - T_c^{4.67}) \qquad (1)$$

where:
q = total heat flux transmitted through the MLI (mW/m^2)
q_c = conductive heat flux transmitted through the MLI (mW/m^2)
q_r = radiative heat flux transmitted through the MLI (mW/m^2)
C_c = conduction constant = 8.95×10^{-5}
C_r = radiation constant = 5.39×10^{-7}
T_h = hot side temperature (K)
T_c = cold side temperature (K)
T_m = mean MLI temperature (K); typically $(T_h + T_c)/2$
ϵ_o = MLI shield-layer emissivity at 300 K = 0.031
N = MLI layer density (layers/cm)
n = number of facing pairs of low-emittance surfaces in the MLI system

In equation (1), MLI conduction is modeled by the first term, and radiation heat transfer is modeled by the second term. In the first term, we see that the conductance of the spacer material is assumed to decrease linearly with absolute temperature as defined by $q_c \propto T_m$, and to increase very steeply with blanket compression as noted by $q_c \propto N^{2.56}$. Radiation heat transfer, modeled by the second term in

equation (1), assumes that the emittance of the MLI surfaces decreases proportional to $T^{0.67}$ as temperature is decreased. This reflects emittance measurements made on aluminum films as reported by Nast [3] and gives $q_r \propto T^{4.67}$.

A weakness in equation (1) is that it is a fit to near-room-temperature experimental data for a particular MLI blanket construction (unperforated double aluminized Mylar with single silk-net spacers used in dewar applications) and does not lend itself to changes in spacer materials, construction differences such as the edge sewing required of spacecraft MLI, or heat transfer differences at ultra low temperatures. To allow these considerations to be incorporated into the MLI heat transfer predictions we have reformulate the terms in equation (1) as described below.

2. Characterization of MLI conduction

2.1 Effect of Number of MLI Layers

As a first step in understanding MLI conduction, it is useful to examine the effect of having multiple MLI layers stacked in series. With the multilayer approach the total temperature difference (ΔT) between the outer blanket layer and the inner blanket layer is divided among the total number of layers. Thus, if the ΔT is distributed equally among 'n' layers, then the total heat transfer per unit area of MLI is given by

$$q_c = k_c \, \Delta T / n \tag{2}$$

where: q_c =   MLI conductive heat flux (mW/m^2)
       k_c =   conductance of a single MLI spacer layer ($mW/m^2 \cdot K$)
       ΔT =   total differential temperature through the MLI blanket (K)
       n   =   number of spacer layers in the MLI

An important conclusion drawn from equation (2) is that the heat flux due to conduction can be made much smaller by increasing the number of spacer layers in the MLI stack. This linear reduction of conduction with increasing numbers of layers is the same as the linear reduction in radiation flux with number of parallel low-emittance layers.

$$q_r = \ 2.835 \times 10^{-5} \, \epsilon \, (T_h^4 - T_c^4) / n \tag{3}$$

where: q_r =   MLI radiative heat flux (mW/m^2)
       ϵ =   emissivity of MLI shield surface, assumed equal for all layers
       T_h =   temperature of hot shield (K)
       T_c =   temperature of cold shield (K)
       n   =   number of pairs of parallel shield surfaces in the MLI

Thus, both conduction and radiation fall proportional to increasing numbers of layers. This makes it somewhat difficult to distinguish between the role of conduction and radiation in experimental measurements of heat transfer through MLI blankets.

2.2 Spacer Material Conductance

Because of the broad temperature range involved in cryogenic MLI systems, from near 300 K to as low as 4 K, it seems desirable, to the extent practical, to also include in the modeling a means of describing the temperature-dependence of the conductivity of the spacer layers themselves. Historically this temperature dependence is not well understood and is most likely a highly nonlinear function of temperature. Figure 1 describes the relative temperature dependence of conductivity of representative spacer materials such as polyethylene terephthalate (Polyester, Mylar, Dacron), Nylon, and Kapton. For this study, and for the lack of a better model, we have chosen to adopt this relative temperature dependence, $\kappa(T)$, as the temperature dependence of the spacers. The MLI conductance (k_c in equation (2)) can then be simplified to a conductance scale factor (k_o) times this relative temperature dependence of the conductivity. Thus,

$$q_c = k_o \, \kappa(T) \, \Delta T / n \tag{4}$$

In equation (4), the term k_o now incorporates the blanket compression term $N^{2.56}$ that is in equation (1) and uses the relative conductance term $\kappa(T)$ in place of the linear temperature dependence assumed by equation (1) for the spacer material conductance.
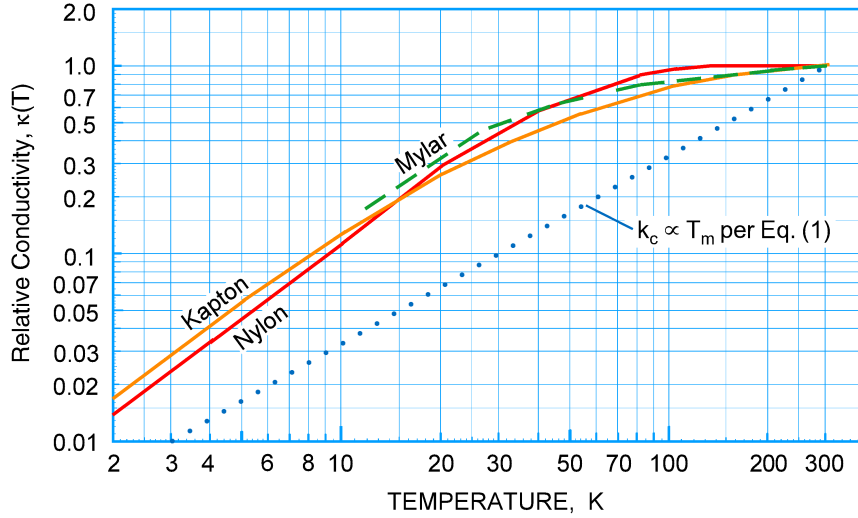
Figure 1. Relative conductivity $\kappa(T)$ data for representative spacer materials.

3. Quantifying MLI Spacer Conductance from Experimental Data

The series nature of heat flow through MLI implies that the total heat transferred between any two adjacent MLI layers anywhere in the stack must be the same. Thus, the sum of radiation plus conduction through any ν layers is the same as the sum of radiation plus conduction through any other number of layers, as noted by

$$q_{Total} \;=\; k_o\,\kappa(T)\,(T_i - T_{i+\nu})\big/\nu \;+\; 2.835\times10^{-5}\,\epsilon\,(T_i^4 - T_{i+\nu}^4)\big/\nu \tag{5}$$

where ν is the number of layers in a convenient subgroup of blanket layers.

One means of extracting conductance data is to solve for the layer-by-layer heat flow through experimentally measured MLI using a set of simultaneous nonlinear equations based on equation (5). By making the heat flow of each subgroup of blanket layers match the measured total heat flow, one can extract the applicable spacer conductance for a given emissivity of the shield layers.

For typical dewar MLI, Lockheed has found that emissivity of the shield layers is best given by

$$\epsilon = 6.8\times10^{-4}\,T^{0.67} \tag{6}$$

Equation (6) follows the $\epsilon \propto T^{0.67}$ dependency noted earlier and gives ϵ_o at $300\,K = 0.031$, the value found by Lockheed to fit the performance of unperforated MLI (no venting holes punched in its surface). With the incorporation of equation (6) for emissivity, and equation (4) and figure 1 for spacer conductance, equation (5) turns into

$$q_{Total} \;=\; k_o\,\kappa(T)\,(T_i - T_{i+\nu})\big/\nu \;+\; 1.928\times10^{-8}\,(T_i^{4.67} - T_{i+\nu}^{4.67})\big/\nu \tag{7}$$

3.1 Spacer Conductance of Broadrange Cryogenic MLI

Here, we define broadrange cryogenic MLI as MLI designed to span from near room temperature on the hot side down to low cryogenic temperatures (4 to 20 K) on the cold side.

As an example of broadrange MLI, consider a 37-layer Lockheed cryogenic dewar blanket made using double-aluminized Mylar (DAM) with single silk-net (SSN) spacers. This particular MLI blanket was tested by Lockheed in an application where it is in direct contact with both a higher-temperature outer wall and a 4 K inner wall [3]. Over the test sequence the outer wall was set at a number of hotside temperatures ranging from 278 K to 40 K, giving multiple cases over which to study blanket conductance. The test data for this MLI are shown in figure 2.

Of interest is that the outstanding performance of this MLI construction at room temperature is seen to drastically fall as the hotside temperature decreases. By 70 K the blanket crosses over to being worse than bare low-emittance surfaces (no blanket), and by 40 K the blanket has nearly four times the heat flux of bare low-emittance surfaces.
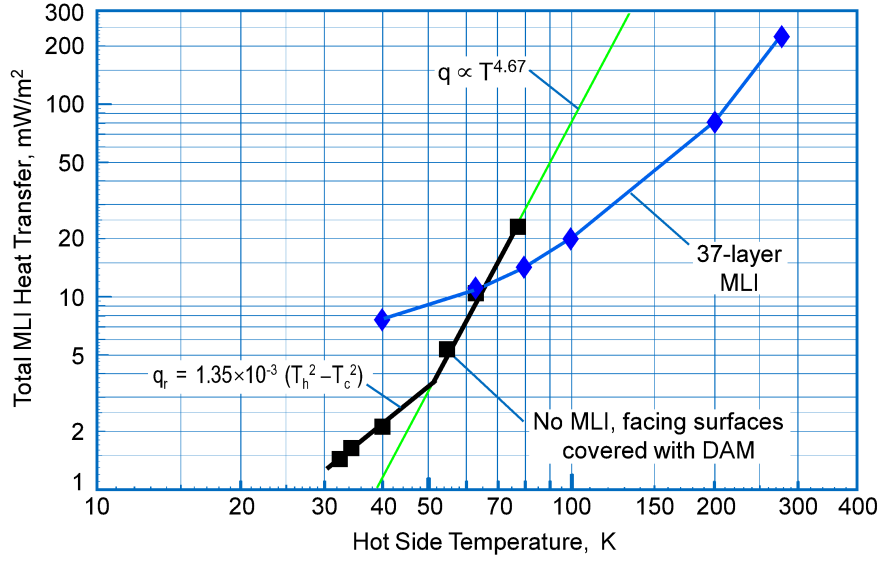
Figure 2. Measured data for performance of 37-layer MLI using double-aluminized Mylar (DAM) and single silk net spacers; also included are low temperature data for the heat flux from opposed walls covered with DAM with no MLI.

First, let us examine the thermal flux calculation for this 37-layer MLI with a 40 K hotside temperature; this provides a measured heat flux of 7.5 mW/m². In this low-temperature region below 50 K, the radiation heat transfer between bare DAM surfaces is seen to deviate from the classical T^4 dependence of equation (5) and follows the trend noted in figure 2. We interpret this as most likely radiation plus some gaseous conduction at these very low heat flux levels. To be complete, we model this behavior as:

$$q_r = 1.35 \times 10^{-3} \, (T_h{}^2 - T_c{}^2) \tag{8}$$

If we substitute this expression for the radiation heat flux term in equation (7) we get

$$q_{Total} = k_o \, \kappa(T) \, (T_i - T_{i+v}) \big/ v \; + \; 1.35 \times 10^{-3} \, (T_i{}^2 - T^2{}_{i+v}) \big/ v \tag{9}$$

Using equation (9), Table 1 presents the results of heat-flux calculations for this 37-layer 40 K MLI based on dividing it into five sub-blankets, each containing the number of layers (v) shown in the table. The solution process requires simultaneously solving five nonlinear equations, one for each sub-blanket, of the form of equation (9) with q_{Total} for each sub-blanket set equal to the measured 7.5 mW/m². By iteratively solving the equation set, one arrives at the temperature distribution shown in the table and a k_o value of around 25 mW/m²·K.

From the calculations it is seen that the heat flux through this 40 K MLI is almost entirely conduction. Thus, at this temperature, the MLI's primary effect is to create a low-conductance thermal short between the outer and inner dewar walls that transmits nearly four times the heat flux that would be transmitted by radiation if the walls were bare low-emittance surfaces.

In contrast to the 40 K application, table 2 provides the thermal flux calculation for the Lockheed 37-layer MLI with a 278 K hotside temperature using the same spacer conductance ($k_o = 25$ mW/m²·K).

Table 1. Calculation of conductance for Lockheed 37-layer MLI with 40 K hotside.

No. Layers (v)	T (K)	ΔT (K)	k_o (mW/m²·K)	q_c (mW/m²)	q_r (mW/m²)	q_{Total} (mW/m²)
cold wall	4.0					
2	11.5	7.5	25	7.5	0.06	7.5
3	16.5	5.0	25	7.5	0.06	7.5
5	22.0	5.5	25	7.5	0.06	7.5
10	30.0	8.0	25	7.5	0.06	7.5
17	40.0	10.0	25	7.5	0.06	7.5

Table 2. Calculation of conductance for Lockheed 37-layer MLI with 278 K hotside.

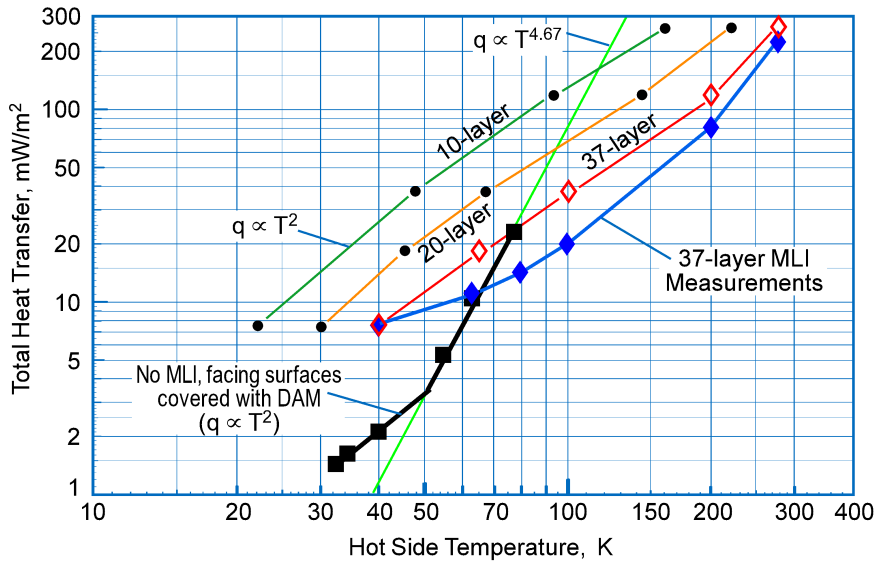| No. Layers (v)	T (K)	ΔT (K)	k_o (mW/m²·K)	q_c (mW/m²)	q_r (mW/m²)	q_{Total} (mW/m²)
cold wall	4.0					
2	38	34	25	252	3	275
3	96	43	25	250	11	275
5	160	64	25	224	57	275
10	220	60	25	132	130	275
17	278	58	25	78	195	275

Figure 3. Modeled performance of the Lockheed 37-layer MLI in comparison with measured heat flux values; modeled results for 10 and 20-layer blankets are also shown.

This is the intended application for this blanket, and its measured heat flux at this temperature (220 mW/m²·K) is extremely low — nearly 25 times lower than with bare low-emittance surfaces.

Note in table 2 that there is substantial radiant heat transfer in the outer layers of the blanket at temperatures above 200 K, but this diminishes to a low level for the layers with temperatures below 100 K. Because radiation at high temperatures is found to follow the Lockheed $T^{4.67}$ temperature dependence, radiation from MLI layers above 50 K was computed using equation (7).

Figure 3 summarizes the results of predicting the heat flux of the Lockheed 37-layer blanket for the full set of hotside temperatures from 278 K to 40 K using the 25 mW/m²·K spacer conductance scale factor. Because temperature data for intermediate layers are also an output of the calculations, additional performance contours have been added showing how similar blankets of 10 layers and 20 layers would perform. Of interest is the fact that the heat flux performance of such a blanket does not vary as $q_{Total} \propto T^4$, as would be predicted by radiation theory alone, but instead follows a much flatter slope corresponding to something like $q_{Total} \propto T^2$.

Figure 4 further illustrates the MLI performance by graphically depicting the increasing role that conduction plays as the hotside temperature is reduced from room temperature to 100 K. Below 100 K the 37-layer MLI is fully dominated by conduction.

3.2 Design of Low Temperature Cryogenic MLI
To improve upon the performance of their broadrange MLI at lower hotside temperatures, Lockheed developed a special 9-layer MLI with three silk-net spacers per DAM layer [2]. The intent of the 9-layer MLI design was to reduce as far as possible the conduction between layers.

Figure 5 describes the performance of this MLI system for a variety of hotside wall temperatures from 75 K down to 27 K. Unlike the 37-layer MLI blanket, these blankets were tested with the outside
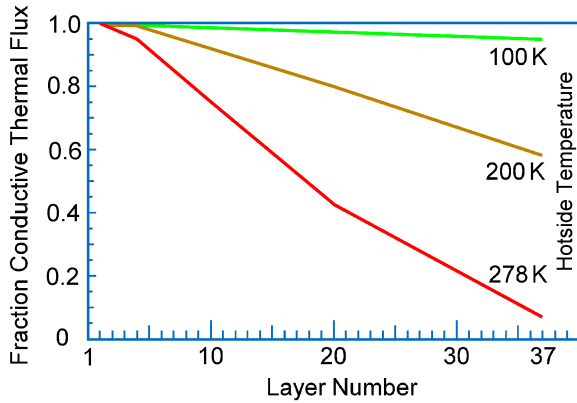
Figure 4. Distribution of radiant and conductive heat transfer through 37-layer MLI as a function of hotside temperature.
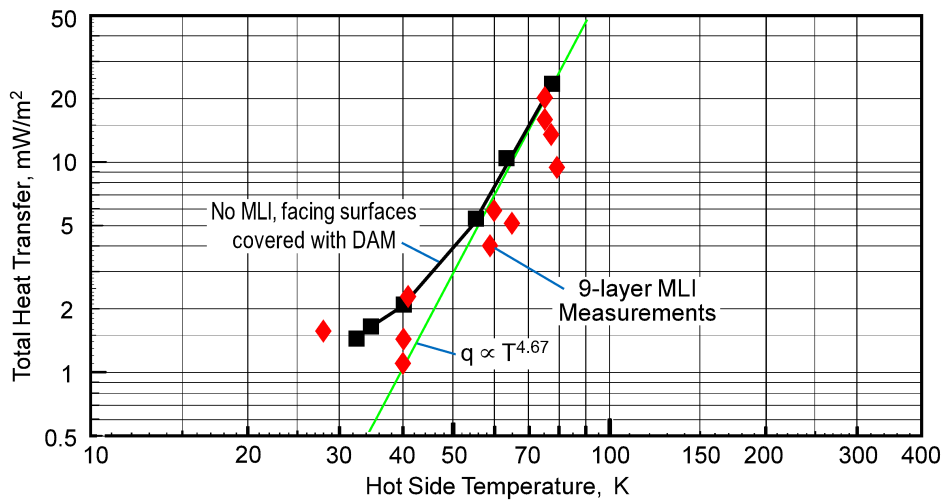

Figure 5. Measured data for performance of Lockheed 9-layer MLI using double aluminized Mylar (DAM) and three silk-net spacers per DAM layer.

MLI layer spaced away from the DAM-covered hotside wall so that no direct conduction (only radiation) existed into the blanket on the hot side. This breaks the direct conductive short provided by the 37-layer blanket between the inner and outer dewar walls. Given the below-50 K region within which these blankets are designed to operate, equation (8) was used to model the radiation flux through the blanket and outer gap; thus, equation (9) was used for the overall blanket modeling.

Table 3 presents the heat-flux computations for the 9-layer MLI with a hotwall temperature of 40 K and a measured total thermal flux of around 1.2 mW/m^2. Note that the outer wall is modeled separately in this table as a low-ϵ radiant source with no conductive link to the blanket outer layer. This gives a depressed blanket outer layer temperature of 30 K, consistent with a factor of two reduction in heat transfer compared with a no-gap configuration.

Table 3. Calculation of conductivity for Lockheed 9-layer MLI with 40 K hotside.

No. Layers (ν)	T (K)	ΔT (K)	k_o (mW/m$^2 \cdot$K)	q_c (mW/m^2)	q_r (mW/m^2)	q_{Total} (mW/m^2)
cold wall	4.2					
1	11.5	8.3	1.5	1.07	0.14	1.2
1	16.5	4.0	1.5	1.07	0.14	1.2
2	21.7	5.4	1.5	1.07	0.14	1.2
2	25.7	4.0	1.5	1.07	0.14	1.2
3	30.0	4.3	1.5	1.07	0.12	1.2
hot wall	40.0	10.0	-	0	1.2	1.2

Table 4. Heatflow calculation for 21-layer Cassini MLI with 328 K hotbox and 87 K coldwall.

No. Layers (ν)	T (K)	ΔT (K)	k_o (mW/m²·K)	q_c (mW/m²)	q_r (mW/m²)	q_{Total} (mW/m²)
cold wall	87		vacuum gap ($\epsilon=1$)			
MLI out surface	121	34	n/a	0	8720	8720
5	167	46	925	8635	85	8720
15	304	137	925	8240	480	8720
1	313	9	925	7613	1107	8720
inner hot box	328	15	vacuum gap ($\epsilon=0.08$)	0	8720	8720

Note that the conductance scale factor for this triple-silk-net blanket (k_o= 1.5 mW/m²·K) is more than an order of magnitude below that of the 37-layer blanket with single silk-net spacers (k_o= 25 mW/m²·K). However, this blanket is seen to still be thoroughly dominated by conduction, with only about 10% of the heat flux transferred by radiation. Additional modeling of this 9-layer blanket for other measured thermal conditions confirm the k_o value of around 1.5 for this blanket construction.

3.3 Spacer Conductance of High Temperature Spacecraft MLI
In contrast to the Lockheed cryogenic dewar MLI, which is carefully assembled one layer at a time to preserve the lowest possible layer density, high temperature spacecraft MLI must be designed to survive launch vibration and launch depressurization loads when attached to spacecraft external surfaces. As a result, it is typically assembled into blankets with sewn seams and is often required to bend around 90º bends. The result is a much higher conductance than is achievable with dewar MLI, where the MLI blanket is launched inside a protective vacuum space just large enough to hold the blanket.

Also, spacecraft MLI is often required to contend with periodic solar illumination on its outer surface, and to serve a micrometeoroid shielding function. These functions can require that it be stood away from its hotside surface and have an external absorptivity/emissivity (α/ϵ) ratio consistent with a tolerable level of solar heating.

To get a feeling for the conductance of representative spacecraft MLI, we apply the same analysis technique to the Cassini MLI data of Lin, Stultz and Reeve [4, 5]. These data are for a cubic aluminum box covered with 0.597 m² of JPL spacecraft MLI and measured in a controlled environment. The MLI construction consisted of an outer layer of second surface aluminized Kapton to provide a moderate external α/ϵ ratio, five layers of crinkled double aluminized Kapton to provide a few high-temperature-tolerant MLI outer layers, 15 layers of double-aluminized Mylar with Dacron-net spacers for the main MLI body, and a final double-aluminized-Kapton inner surface for robustness. Over the test sequence the aluminum cube was set at hotside temperatures of 295 K (22ºC) and 323 K (50ºC), and the outer radiation sink was set at temperatures of 87 K and 170 K. As with the Lockheed tests, this study provided multiple cases over which to evaluate the MLI's conductance. However, in contrast to the Lockheed 37-layer blanket, this blanket passed a measured heat flux of around 6000 mW/m²·K at 300 K, 27 times that of the Lockheed 37-layer blanket and roughly equal to that of a single bare-aluminum low emittance shield.

An example calculation for the Cassini MLI is shown in table 4 for the case with an 87 K external radiation sink temperature and a 328 K hotside box temperature. Note that the derived conductance (k_o) is 925 mW/m²·K. This is 37 times higher than the Lockheed 37-layer dewar MLI conductance, and over 600 times higher than that for the Lockheed low-temperature 9-layer dewar MLI. Analysis of additional test cases provided k_o values ranging from 800 to 1100 mW/m²·K. Note also that, despite the high temperatures involved, the heat transfer through the Cassini spacecraft MLI is dominated by conduction; this reflects the very high conductance of this construction.

4. MLI Conductance Summary
Figure 6 summarizes the MLI conductance curves derived from the above analyses. It is clear from the three-order-of-magnitude range of values that MLI conductance is a high-uncertainty parameter in MLI performance. It is particularly important to note from the above analyses that conductance governs the thermal performance of both high-temperature spacecraft MLI as well as low-temperature cryogenic
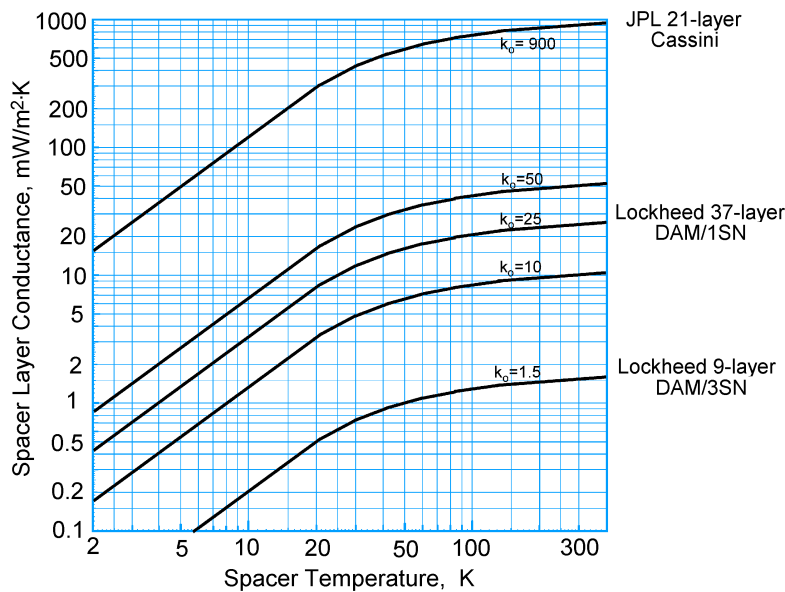
Figure 6. MLI conductance $k_o \kappa(T)$ between two parallel shield layers separated by a spacer layer versus the temperature of the spacer layer for various MLI constructions.

MLI. For both of these temperature extremes, MLI emittance is found to play a secondary role to spacer conductance in establishing MLI thermal effectiveness. Thus, MLI performance is critically dependent on the achieved MLI conductance.

If we examine the thermal role of conduction-dominated MLI, we find that it reduces heat flow by blocking radiation and creating a low thermal conductance between its radiation-heated outer surface and its opposite cold surface. It also lowers the net radiation heat exchange to its hotside surface by having its hotside surface rise up in temperature and approach the temperature of the hotside radiating source. The lower the conductance of the MLI blanket spacers, the lower the conduction through the blanket, and the higher the hotside temperature, which reduces the net absorbed radiation.

Because conduction-dominated MLI can function similar to a floating thermal shield with emittance properties similar to that of bare low-emittance surfaces, its performance benefits well from being spaced away from all surfaces so that it can achieve its optimum shielding temperature —generally close to the hotside radiating source temperature. With non-conduction-dominated MLI, this seeking out of the optimum floating-shield temperature is performed automatically by the various MLI layers of these blankets, which are only weakly tied together conductively.

6. Acknowledgment

7. References

[1]   Kutzner K, Schmidt F and Wietzke I 1973 Radiative and conductive heat transmission though super-insulations—experimental results for aluminum coated plastic foils *Cryogenics* **13** n.7 pp 396-404

[2]   Keller CW, Cunnington GR and Glassford AP 1974 *Final Report - Thermal Performance of Multi-layer Insulations* NASA Contractor Report CR-134477 Lockheed Missiles & Space Co

[3]   Nast TC 1993 A review of multilayer insulation, theory, calorimeter measurements, and applications *Recent Advances in Cryogenic Engineering* vol 267 ASME HTD ed JP Kelley and J Goodman (New York: Amarican Society of Mehanical Engineers) pp 29-44

[4]   Lin EI, Stultz JW and Reeve RT 1995 Test-derived Effective Emittance for Cassini MLI Blankets and Heat Loss Characteristics in the Vicinity of Seams *AIAA paper 95-2015* 30th AIAA Thermophysics Conference 19-22 June 1995 San Diego CA

[5]   Lin EI and Stultz JW 1995 Cassini MLI Blankets High-Temperature Exposure Tests *AIAA paper 95-0633* 33rd Aerospace Sciences Meeting 9-12 January 1995 Reno NV